THE JOURNAL OF PHYSICAL CHEMISTRY C

Article

pubs.acs.org/JPCC

Graphitic Carbon Nitride Supported Catalysts for Polymer Electrolyte Fuel Cells

Noramalina Mansor,[†] A. Belen Jorge,[‡] Furio Corà,[‡] Christopher Gibbs,[†] Rhodri Jervis,[†] Paul F. McMillan,[‡] Xiaochen Wang,[‡] and Daniel J. L. Brett*[,†]

[†]Electrochemical Innovation Lab, University College London, London WC1E 7JE, United Kingdon

[‡]Department of Chemistry, University College London, London WC1H 0AJ, United Kingdom

ABSTRACT: Graphitic carbon nitrides are investigated for developing highly durable Pt electrocatalyst supports for polymer electrolyte fuel cells (PEFCs). Three different graphitic carbon nitride materials were synthesized with the aim to address the effect of crystallinity, porosity, and composition on the catalyst support properties: polymeric carbon nitride (gCNM), poly(triazine) imide carbon nitride (PTI/Li^+Cl^-), and boron-doped graphitic carbon nitride (B-gCNM). Following accelerated corrosion testing, all graphitic carbon nitride materials are found to be more electrochemically stable compared to conventional carbon black (Vulcan XC-72R) with B-gCNM support showing the best stability. For the supported catalysts, Pt/PTI-Li^+Cl^- catalyst exhibits better durability with only 19% electrochemical surface area (ECSA) loss versus 36% for Pt/Vulcan after 2000 scans. Superior methanol oxidation activity is observed for all graphitic carbon nitride supported Pt catalysts on the basis of the catalyst ECSA.

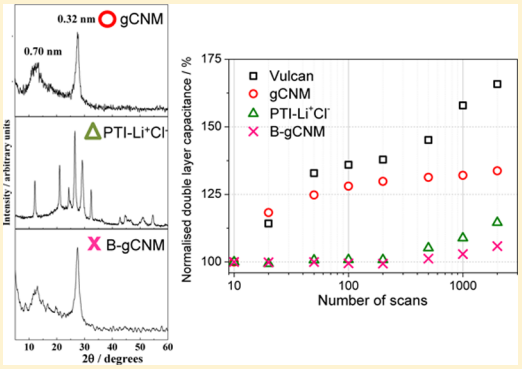

1. INTRODUCTION

Among the various types of fuel cells, polymer electrolyte fuel cells (PEFCs) have attracted the most attention for transportation and portable applications. Advantages include the following: rapid start-up and shut down, low temperature operation (~80 °C), high power density, and fully solid state components. Current state-of-the-art technology uses platinum (Pt) or platinum alloys supported on carbon for both anode and cathode electrodes. It is estimated that the catalyst layers contribute to as much as 39% of the total fuel cell stack cost,[1] making it one of the major challenges for PEFC commercialization. In order to meet the U.S. Department of Energy (DOE) targets for 2015, it is necessary to reduce the amount of Pt catalyst used by three-quarters, while ensuring the same performance.[2] Another major challenge is insufficient durability; current state-of-the art performance under realistic operating conditions is just half of the target set by the DOE.[2] It is generally accepted that catalyst activity and durability depends on Pt particle size and dispersion (which can be affected by the support material), as well as the interaction between the catalyst particle and the support.[3,4] Therefore, the support plays a crucial role for optimal catalyst performance. The most widely used catalyst support is carbon black Vulcan XC-72R, which has high surface area and good electrical conductivity. However, Pt particles can get "buried" inside the pores and hence reduce the active triple-phase boundary accessible for electrochemical reaction. Furthermore, Vulcan XC-72R is electrochemically unstable at high potential, leading to corrosion after extended operation in acidic media and varying potentials. As the carbon corrodes, Pt nanoparticles agglomerate into larger particles and/or detach from the support material, consequently reducing the electrochemical surface area (ECSA) and catalytic activity.[5,6]

To solve this issue, much effort has been directed toward the development of alternative, chemically stable catalyst supports. In recent years, numerous conductive ceramics or oxide containing composites have been studied; these include ITO, WO_3, TiO_2, CeO_2 and CeO_2–ZrO_2, WC, Ti_4O_7, NbO_2 or Nb_2O_5, TiN, TiB_2, and SiC.[7−17] Various graphitized carbon support materials with special pore structures have also been explored, such as carbon nanotubes (CNTs), nanofibers (CNFs), nanohorns (CNHs), and nanocoils (CNCs).[18−26] Despite having promising performance and durability, there are concerns over their costly and complex synthesis methods.[27−32] The graphitic structure has been shown to be effective at increasing durability; however, its inert surface has a limited amount of active sites where the Pt nanoparticle can stably anchor. These are often associated with structural electronic defects that yield higher interaction energy with the metal nanoparticle. A reasonable balance between catalyst dispersion and catalyst−support interaction is necessary to meet the fuel cell performance requirement.

An emerging trend is to dope the carbon support materials with oxygen or nitrogen, which act as "tethers" or "anchors" by increasing the interaction of the catalyst with the supporting

Received: December 20, 2013
Revised: March 2, 2014
Published: March 5, 2014

   dx.doi.org/10.1021/jp412501j | J. Phys. Chem. C 2014, 118, 6831−6838

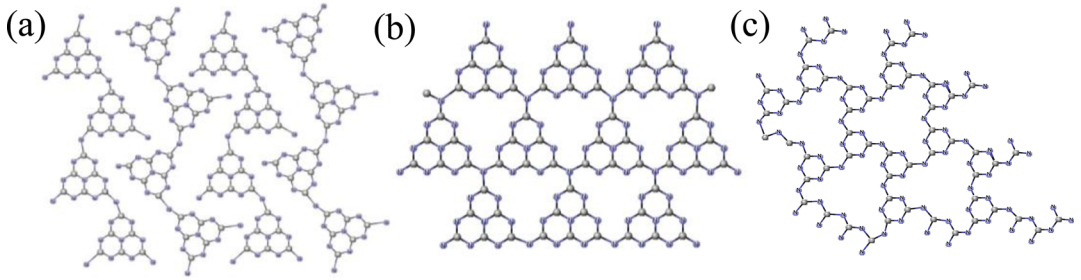

Figure 1. Structural motifs found in graphitic carbon nitrides: (a) Liebig's melon ($[C_6N_7(NH_2)(NH)]_n$) contains zigzag chains of heptazine (tri-s-triazine) units linked by bridging −NH− groups and decorated on their edges by N−H groups, (b) fully condensed C_3N_4 layer based on heptazine units, and (c) graphitic carbon nitride based on triazine ring units.

materials, which leads to increased Pt nanoparticle dispersions.[33−35] Unfortunately, surface oxygen functional groups on carbon are known to reduce the durability of fuel cell catalysts by promoting carbon corrosion.[36] On the other hand, a growing body of literature suggests that the presence of nitrogen in carbon supports improves durability, as well as enhancing the intrinsic catalytic activity for both oxygen reduction reaction (ORR) and methanol oxidation reaction (MOR).[37−42] The incorporation of nitrogen into carbon leads to a reduction in detrimental surface oxygen groups and thus provides enhanced tolerance toward oxidation.[33] The role of the N-surface species in catalytic enhancement is less studied and has only been hypothesized based on experimental observation and physicochemical reasoning. For example, it was suggested that C−N defects near the catalyst−particle interface adsorb oxygen containing intermediates that would otherwise block catalyst active sites, and thereby facilitate their removal and increase the rate of electrochemical reaction.[33,43] It has been shown that the N-dopant alters the catalyst electronic structure, resulting in a higher binding energy, which may decrease the specific interaction between the Pt nanoparticles and poisoning intermediates.[44] This is further supported by an X-ray photoelectron spectroscopy (XPS) study and theoretical calculations, where it was observed that Pt nanoparticles nucleate strongly and experience a strong "tethering" effect to N atoms.[45,46] N-doped carbon materials also have higher specific capacitance, suggesting the presence of additional charged species within the Helmholtz layer, which might provide sites for surface groups to participate in the removal of strongly adsorbed poisoning intermediates.[47]

Given the potential of N-doped carbon materials, graphitic carbon nitride material was chosen as a suitable candidate for a catalyst support in this study. Polymeric solids with high N:C ratios formed by reactions of nitrogen-rich molecules were first reported by Berzelius and later studied by Liebig, Franklin, Pauling, and others.[48,49] A fully condensed end member has the composition C_3N_4 with a planar structure related to graphite or graphene. However, most graphitic carbon nitrides are composed of C and N, along with residual amounts of H, and they are attracting new interest due to their unique structural and optoelectronic properties.[50−55] The structures are based on triazine (C_3N_3) or heptazine (C_6N_7) ring units linked by −N = or −NH− bridges to form sheets or zigzag chains of monomer units linked by hydrogen bonds to give a 2D array. Typical examples include Liebig's melon, melem, or highly condensed $C_xN_yH_z$ graphitic structures formed by continued elimination of NH_3 component (Figure 1a−c). Recent discussions of graphitic carbon nitride structures and their properties have been based mainly on polymerized heptazine models that are shown to more thermodynamically stable,[50−52] but structures based on condensation of s-triazine rings can also be produced under different synthesis conditions, and both structure types may be present.

Graphitic carbon nitrides are semiconductors with an intrinsic band gap near 2.7 eV and optical absorption extending into the visible range.[56,57] These materials exhibit catalytic and photocatalytic activity and are also of interest for their intercalation, ion exchange, and redox properties.[56−63] Because of their high nitrogen content, tunability reminiscent of polymer chemistry, and facile synthesis procedure, they may provide a good balance between activity, durability, and cost in PEFC operation. However, literature data on these applications are limited. Recent studies show that graphitic carbon nitride−carbon composites could provide comparable ORR catalytic activity to that achieved by commercial Pt/C in alkaline electrolyte with enhanced durability and high carbon monoxide (CO) tolerance.[64] Although nitrogen in N-doped graphite/graphene introduces a charge carrier (n-type polaron), this charge is not necessarily localized on the nitrogen. In the case of graphitic carbon nitride materials, they are stoichiometric materials and contain abundant Lewis acid and base sites (terminal and bridging NH− groups and lone pairs of N in triazine/heptazine rings, respectively) that are potential anchoring sites for Pt as well as adsorption sites for CO. To our knowledge, the first application of graphitic carbon nitride as a catalyst support can be attributed to Yu et al. in 2007 for the direct methanol fuel cell (DMFC) operation.[65] It was shown that PtRu supported on graphitic carbon nitride in DMFC exhibits 78−83% higher power density than on Vulcan XC-72.

Previously, it was shown that Pt deposited on graphitic carbon nitride is more stable than commercial Pt/Vulcan under acidic accelerated carbon corrosion protocol (after 1000 scans) and has higher methanol oxidation activity per electrochemical surface area.[66] In this study, three different graphitic carbon nitride materials (polymeric carbon nitride, crystalline poly(triazine) amide, and boron-doped graphitic carbon nitride) were prepared, and their electrochemical durability was investigated in comparison to conventional carbon black, Vulcan XC-72. Pt nanoparticles were deposited on each material, and their electrochemical properties and potential applications in PEFC were investigated.

2. EXPERIMENTAL SECTION

2.1. Synthesis of Graphitic Carbon Nitride Materials.

Polymeric carbon nitride (gCNM) was prepared by thermolysis and condensation reactions of a 1:1 molar ratio mixture of dicyandiamide (DCDA, $C_2N_4H_4$) and melamine ($C_3N_6H_9$) at 550 °C. A finely ground sample was loaded in an alumina boat into a quartz tube in a tubular furnace under nitrogen flow. The temperature was raised to 550 °C at 5 °C/min for 15 h.

dx.doi.org/10.1021/jp412501j | J. Phys. Chem. C 2014, 118, 6831−6838

Crystalline poly(triazine)imide (PTI/Li^+Cl^-) was synthesized from DCDA in molten eutectic LiCl/KCl (45:55 wt %) mixtures heated at 400 °C under N_2 (g) for 6 h and then sealed under vacuum and heated to 600 °C for 12 h.

B-doped graphitic carbon nitride (B-gCNM) was prepared by using ionic liquids. In a typical synthesis, 1-butyl-3-methyl-imidazolium tetrafluoroborate ($BmimBF_4$) was dissolved in water and stirred for 5 min. Then DCDA was added, and the mixture was heated at 100 °C in an oil bath until the water completely evaporated. The resulting solid was then heated in an alumina crucible for 2 h at 350 °C and kept at this temperature for 4 h. Then, the temperature was raised to 550 °C for another 4 h and finally cooled to room temperature.

2.2. Deposition of Pt Catalyst. The Pt catalyst was deposited onto gCNM using the ethylene glycol reduction method. Ground gCNM (0.09 g) was dispersed in 200 mL of ethylene glycol (Fisher Scientific), and chloroplatinic acid (39.82% Pt basis, 0.1507 g, Sigma Aldrich) was added to the suspension. The mixture was stirred for 4 h under inert atmosphere and then heated to 140 °C for 3 h, resulting in a dark brown mixture. The solid product was collected via vacuum filtration and dried at 60 °C in a vacuum oven. The Pt loading was 40 wt % for Pt/gCNM and 20 wt % for Pt/PTI-Li^+Cl^- and Pt/B-gCNM.

2.3. Structural and Compositional Characterization of Support and Catalyst. C, N, H analyses for gCNMs were performed using a Carlo-Erba EA1108 system. SEM was performed with a JEOL JSM-6301F field emission imaging system at 5 kV. TEM images were taken using a JEOL TEM1010 instrument operating at 80 kV and HRTEM images were taken using a JEOL TEM2010 instrument operating at 200 kV. The X-ray diffraction data were obtained using a Bruker-AXS D4 system for the support materials and STOE powder diffractometer for the supported catalyst materials. BET measurements were carried out using a Micrometrics ASAP 2420 Surface Area/Porosity Analyzer.

2.4. Electrochemical Characterization. The electrochemical measurements were carried out in a conventional three-electrode cell connected to an Autolab PGSTAT32 potentiostat. A glassy carbon (GC) electrode with a surface area of 0.196 cm^2 was employed as a working electrode, a Pt mesh was used as a counter electrode, and a hydrogen reference electrode (Gaskatel), joined to the main chamber via a Luggin capillary, was used as a reference electrode. A catalyst ink of 1.4 mg mL^{-1} was obtained by dispersing the catalyst in a mixture of acetone, isopropyl alocohol, and Nafion ultrasonically for 1 h. The ink was deposited on the GC and dried at room temperature, resulting in a loading of 35 μg cm^{-2}. The working electrode was electrochemically cleaned prior to each measurement via potential cycling between 0 and 1.2 V for 10 cycles, or until a steady state was reached, at a scan rate of 20 mV s^{-1}. All electrochemical measurements were carried out at 25 °C in 0.1 M $HClO_4$, except for MOR which was carried out in 1 M CH_3OH + 0.1 M $HClO_4$. The electrolyte was thoroughly purged with N_2 for 30 min prior to every experiment. All chemicals used were analytical grade, and solutions were prepared with deionized water (Millipore, 18.2 MΩ·cm)

2.5. Carbon Corrosion. An accelerated start−stop cycling protocol was used for the carbon corrosion test. One cycle involves applying a voltage hold at 1.0 V for 30 s followed by two sequences of voltage cycling between 1.0 and 1.5 at 0.5 V s^{-1}. The change in cyclic voltammogram (capacitance and electrochemical surface area) was monitored after 1, 10, 20, 50, 100, 200, 500, 1000, and 2000 cycles. The tests were conducted at 60 °C in N_2 purged 0.1 M $HClO_4$.

3. RESULTS

3.1. Characterization of Support Materials. In this study, different graphitic carbon nitride phases were prepared with the aim to address the effect of catalyst support properties such as *crystallinity, porosity*, and *composition* on the electrochemical performance in PEFC. Polymeric carbon nitride was prepared using a typical method of thermolysis and condensation. Electronically modified graphitic carbon nitride with high porosity was prepared using ionic liquid under the same conditions, whereas highly crystalline graphitic carbon nitride was prepared via ionothermal method.

3.1.1. gCNM. Layered carbon nitride was prepared by thermolysis and condensation reactions of 1:1 molar ratio mixtures of dicyandiamide ($C_2N_4H_4$) and melamine ($C_3N_6H_9$) at 550 °C for 15 h.[18] Finely ground samples were heated in a tubular furnace under N_2 flow at 5 °C/min and allowed to cool to room temperature before being removed. Upon heating, the condensation process takes place by removal of NH_3 species leading to materials with different C:N:H stoichiometry depending on the synthesis temperature.[18] Elemental analysis revealed that the material had a composition of $C_{3.0}N_{5.2}H_{1.6}$.

A typical X-ray diffraction pattern (XRD) is shown in Figure 2a. The strong peak at ∼27.5° 2θ corresponds to a repeat distance of ∼0.32 nm that correlates with the 002 reflection usually observed for graphitic materials. The feature around 12.5° 2θ corresponds to an in-plane repeat distance of 0.70 nm that matches with the dimensions of polyheptazine or polytriazine structures within the layers.

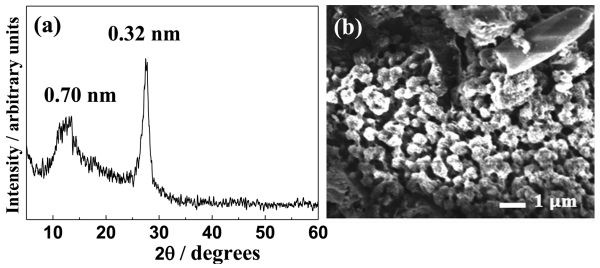

Figure 2. X-ray diffraction pattern (a) and SEM image (b) of a typical layered carbon nitride prepared by thermal condensation of DCDA/melamine 1:1 molar ratio.

Scanning electron microscope (SEM) examination (Figure 2b) indicated that gCNM exhibits a latticework of interlocking planar microstructures with individual layer thicknesses on the order of 2−3 nm that give rise to porous aggregates with pore sizes on the order of a few nanometers. This material is not highly condensed, and its structure is believed to be close to that of Liebig's melon. The aggregates are fused together to give rise to much larger pores (1−2 μm) in the resulting solid. The BET measurements showed a surface area of 28 m^2 g^{-1}.

3.1.2. PTI-Li^+Cl^-. Poly(triazine) imide carbon nitride (PTI-Li^+Cl^-) was prepared using an ionothermal route. This method allowed us to obtain a highly crystalline carbon nitride using relatively mild conditions. In a typical synthesis, DCDA was mixed with a eutectic mixture of LiCl/KCl (45:55 wt %) and heated at 400 °C for 6 h under N_2 (g) followed by a thermal treatment under high vacuum at 600 °C for 12 h. The PTI-Li^+Cl^- compound exhibits a sharp series of peaks in the X-ray diffraction

dx.doi.org/10.1021/jp412501j | J. Phys. Chem. C 2014, 118, 6831−6838

pattern consistent with a $P6_3cm$ unit cell (Figure 3a).[67,68] The hexagonal symmetry of the PTI-Li^+Cl^- can be clearly seen in the

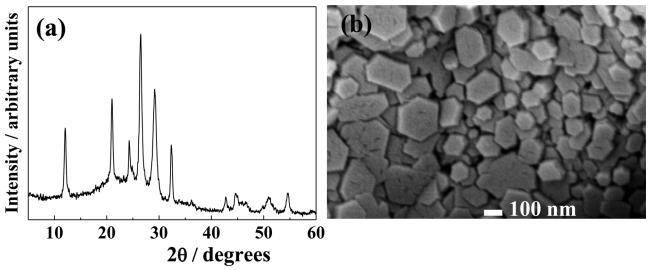

Figure 3. X-ray diffraction pattern (a) and SEM image (b) of a poly(triazine)imide carbon nitride prepared by ionothermal route.

SEM images of the hexagonal-shaped crystallites (Figure 3b). This material is a triazine-based $(C_3N_3)_2(NH)_3$.LiCl structure with Li^+ and Cl^- intercalated both within and between the graphitic layers.[68]

3.1.3. B-gCNM. 1-Butyl-3-methylimidazolium tetrafluoroborate ($BmimBF_4$) ionic liquid was used to modify the electronic structure of gCNM by substituting C ($[He]2s^22p^2$) by B ($[He]2s^22p^1$). $BmimBF_4$ acts also as soft-template inducing higher porosity in the material.[56] The X-ray diffraction pattern (Figure 4a) is dominated by the (002) interlayer-stacking

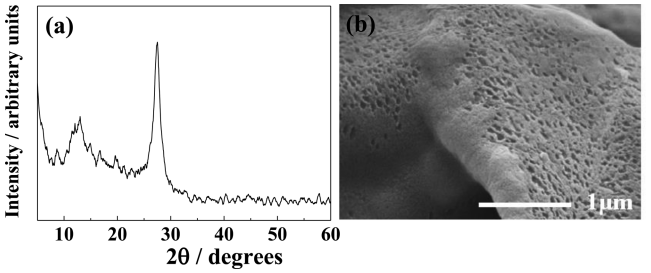

Figure 4. X-ray diffraction pattern (a) and SEM image (b) of B-gCNM doped with 10 wt % B.

reflection usually observed in gCNMs. The higher porosity of B-gCNM compared to gCNM and PTI-Li^+Cl^- is clearly seen in the SEM images (Figure 4b). A homogeneous porosity with pores of about 50−75 nm were detected. These pores were considerably smaller than those observed in gCNM.

3.2. Characterization of Supported Catalysts. Platinum was deposited onto the supports via the ethylene glycol method. The materials were characterized via XRD and transmission electron microscopy (TEM). The XRD patterns (Figure 5a−d) confirm the presence of platinum in each sample as characterized by the peaks at 39.8° 2θ and 46.5° 2θ corresponding to Pt 111 and 200 reflections, respectively. The TEM images shown in Figure 6a−d indicate varying extents of Pt nanoparticle dispersion in each sample, with large agglomeration seen in all samples except for the commercial catalyst.

The average Pt crystallite sizes calculated using the Scherrer equation and the particle size estimated from TEM images are summarized in Table 1. All Pt on graphitic carbon nitride materials have larger particle sizes (4.2−8.0 nm) compared to commercial Pt/Vulcan (3.5 nm). This is due to the agglomeration in all the samples, indicating that the method used for catalyst deposition is not optimized.

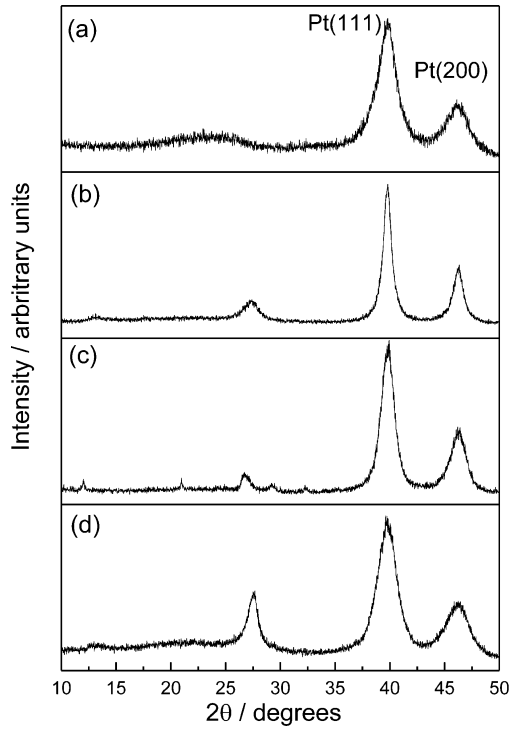

Figure 5. X-ray diffraction pattern of supported Pt electrocatalysts: (a) Pt/Vulcan, (b) Pt/gCNM, (c) Pt/PTI-Li^+Cl^-, and (d) Pt/B-gCNM. Peaks for nanocrystalline Pt are significantly stronger than gCNM features.

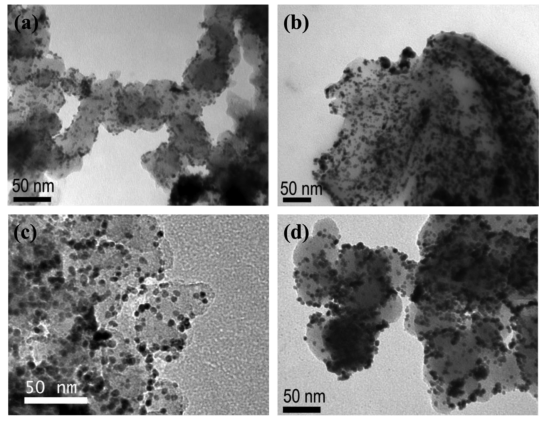

Figure 6. TEM images of (a) Pt/Vulcan, (b) Pt/gCNM, (c) Pt/PTI-Li^+Cl^-, and (d) Pt/B-gCNM.

Table 1. Average Particle and Crystallite Size of Supported Pt Catalysts

	particle size[a] (nm)	crystallite size[b] (nm)	conductivity[c] (S cm^{-1})
Pt/Vulcan	3.5	3.6	~200
Pt/gCNM	8.0	8.9	6.7×10^{-2}
Pt/PTI-Li +Cl^-	6.4	5.8	–
Pt/B-gCNM	4.2	3.3	7.7×10^{-2}

[a]Estimated from TEM image based on the average of 100 particles. [b]Calculated from 111 signal widths of XRD using the Scherrer equation. [c]Conductivity of support materials.

3.3. Durability Studies. The stability of the carbon nitrides was determined by observing the change in double-capacitance

dx.doi.org/10.1021/jp412501j | J. Phys. Chem. C 2014, 118, 6831−6838

in the cyclic voltammetry measurements while performing the carbon corrosion test. The capacitance was calculated at 0.40 V and normalized to the 10th scan. Capacitance increases with the number of scans due to an increase in surface area and concentration of hydrophilic carbon corrosion products with oxygen functionalities at the surface of the carbon support.[69,70] The presence of oxygen functionalities reduces the durability of PEFC catalysts by promoting carbon corrosion. In addition, a more hydrophilic surface may affect water management in fuel cells and potentially contribute to performance instability and variability. Figure 7 displays the degree of corrosion behavior/

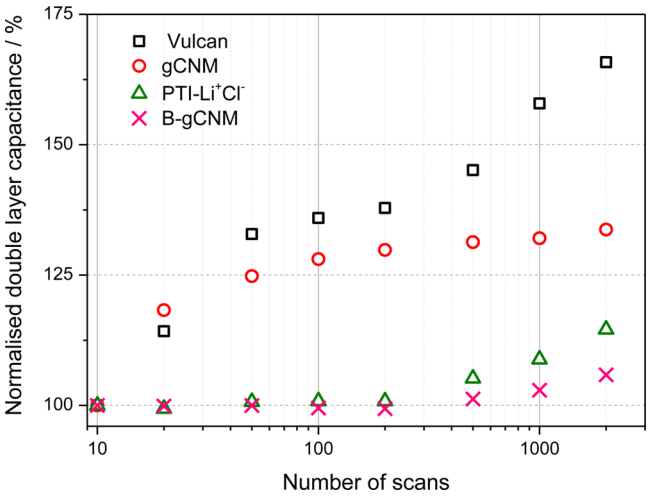

Figure 7. Change in double-layer capacitance (calculated at 0.40 V) of the support materials as a result of accelerated carbon corrosion cycling.

surface modification of graphitic carbon nitride materials, in comparison to a commercial Vulcan carbon support. After 2000 cycles, all materials exhibit a higher degree of tolerance to cycling, compared to commercial carbon black (Vulcan), with B-gCNM showing the best tolerance at only a 6% increase in capacitance at the end of the cycle.

All carbon nitride supported Pt catalysts have lower initial electrochemical surface area (ECSA) compared to commercial Pt catalyst.[71] This is due to higher degree of agglomeration and larger particle size, as shown in Figure 6. This also indicates that each graphitic carbon nitride material has a different ability to accommodate catalyst particles. In addition, carbon nitride materials have 1 order of magnitude less BET surface area compared to Vulcan carbon, and hence the same mass percentage loading of Pt nanoparticles on Vulcan carbon would result in higher Pt particle density on graphitic carbon nitride.

The durability of the materials in the presence of Pt nanoparticles was evaluated using the same accelerated protocol, with CV and ECSA recorded at regular intervals as part of the diagnostic (Figure 8). The decrease in ECSA is believed to be due to platinum agglomeration and dissolution as a result of substrate corrosion.[4,70] At the end of the 2000 cycles, commercial Pt/Vulcan exhibits a 36.3% decrease in ECSA (Table 2). Pt/gCNM and Pt/B-gCNM show higher ECSA loss at 81.0% and 100% loss, respectively, despite each support having higher degree of corrosion tolerance, as displayed in Figure 7. Pt/PTI-Li^+Cl^- exhibits the highest durability at only 19.3% ECSA loss. In addition, it is also observed that graphitic carbon nitride supported Pt catalysts with higher initial ECSA exhibit higher electrochemical durability, indicating there is a link between

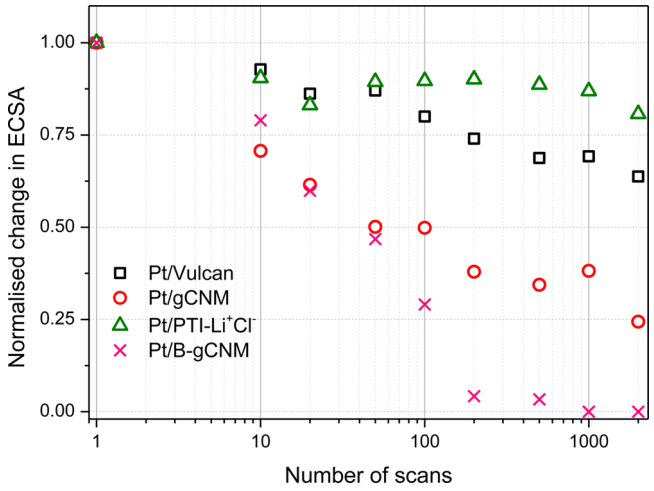

Figure 8. Change in ECSA (calculated from hydrogen adsorption/desorption) of the supported Pt electrocatalsysts as a result of accelerated carbon corrosion cycling.

Table 2. ECSA of Supported Pt Electrocatalysts before and after the Accelerated Carbon Corrosion Cycling (2000 Cycles)

	initial ECSA (m^2 g^{-1})	final ECSA (m^2 g^{-1})	ECSA loss (%)
Pt/Vulcan	28.6	18.2	36.3
Pt/gCNM	5.7	1.1	81.0
Pt/PTI-Li^+Cl^-	15.9	12.8	19.3
Pt/B-gCNM	1.9	0	100

good metal−support interaction and durability. Support material that provides strong adsorption and anchoring sites for the Pt nanoparticles will increase particle dispersion and limit leaching and agglomeration processes during the accelerated test.[33]

3.4. Electrocatalytic Activity. The catalytic activities of graphitic carbon nitride supported Pt catalysts were investigated in 1 M methanol + 0.1 M $HClO_4$ solution at 25 °C. Figure 9 compares the methanol oxidation peak of each supported catalyst. It is generally accepted that low overpotential and high peak current density are an indication of good methanol oxidation reaction (MOR) activity. The current density is normalized to the ECSA of each respective material due to the inherent differences in ECSA. The results are summarized in Table 3. All graphitic carbon nitride supported catalysts exhibit lower overpotential and higher peak current density compared to Pt/Vulcan. In addition, Pt/PTI-Li^+Cl^- exhibits the lowest overpotential whereas Pt/B-gCNM has the highest peak current density. MOR overpotential may be influenced by particle size effects: smaller Pt nanoparticles enhance the oxidation of poisoning intermediates and, hence, decrease the overpotential.[72,73] Given the difference in Pt particle size in all materials with Pt/Vulcan having the smallest particle size, particle size effect can be eliminated from this observation. This suggests that the presence of nitrogen on/within the support material could lead to intrinsic MOR catalytic enhancement. However, more work is needed to optimize the particle dispersion and ECSA. Furthermore, each of the graphitic carbon nitride materials has different structural properties and therefore would require a different synthesis approach.

dx.doi.org/10.1021/jp412501j | J. Phys. Chem. C 2014, 118, 6831−6838

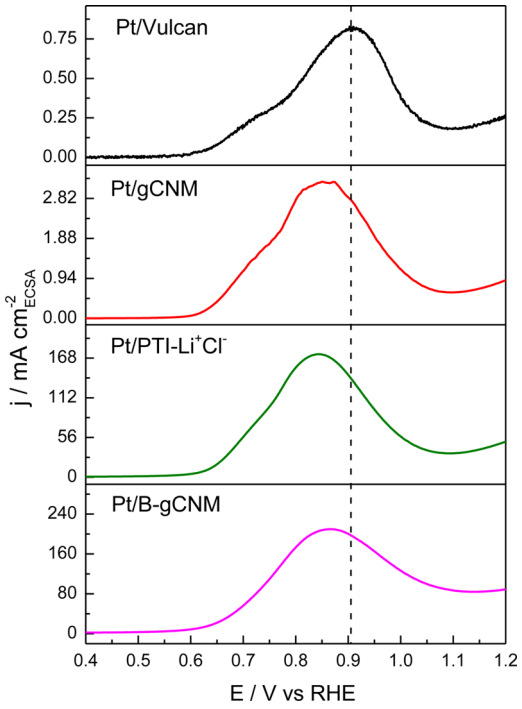

Figure 9. Methanol oxidation reaction of supported Pt electrocatalysts in 1 M CH_3OH + 0.1 M $HClO_4$ at 25 °C with a scan rate of 2 mV s^{-1}.

Table 3. Methanol Oxidation Peak Potential (E_{peak}) and Maximum Methanol Oxidation Reaction Current Density (j_{max}) of Supported Pt Electrocatalysts in 1 M CH_3OH + 0.1 M $HClO_4$ at 25 °C

	E_{peak} (V)	j_{max} (mA cm^{-2}_{ECSA})
Pt/Vulcan	0.903	0.821
Pt/gCNM	0.850	3.21
Pt/PTI-Li^+Cl^-	0.842	174
Pt/B-gCNM	0.858	209

4. CONCLUSION

For the first time, three different graphitic carbon nitride materials (polymeric gCNM, PTI-Li^+Cl^-, and B-doped gCNM) were prepared and tested as catalyst support materials for PEFCs. The results show that all graphitic carbon nitride materials prepared in this study exhibit significantly improved durability compared to commercial carbon black (Vulcan XC-72R) and, therefore, are promising catalyst support materials for PEFC applications. Interestingly, B-gCNM and PTI/Li^+Cl^- exhibit the highest stability. As shown on the X-ray diffraction patterns, B-gCNM and PTI/Li^+Cl^- are more crystalline than Vulcan and gCNM, suggesting that crystallinity may play an important role in the stability of the material against carbon corrosion. This also suggests that the presence of dopants such as boron in B-gCNM, and Li^+ and Cl^- in PTI/Li^+Cl^-, may enhance the stability of the support materials.

The durability of graphitic carbon nitride supported Pt electrocatalysts is highly dependent on the initial ECSA. The Pt/B-gCNM, with the lowest ECSA of all carbon nitride supported catalyst, exhibits the lowest durability with a loss of 100% after 2000 cycles. The Pt-PTI/Li^+Cl^- has the best durability of all Pt-supported catalyst with an ECSA loss of only 19% after 2000 scans. This value is even lower than Pt/Vulcan with an ECSA loss of 36%. In addition, all graphitic carbon nitride supported Pt electrocatalysts have higher methanol oxidation activity per ECSA, compared to Pt/Vulcan.

This work shows that graphitic carbon nitrides are promising catalyst supports that can potentially replace conventional carbon support. They exhibit higher stability against corrosion and higher methanol oxidation reaction activity. The performance of PTI/Li^+Cl^- is highly encouraging, and further research is already being developed to optimize catalyst particle dispersion and utilization.

AUTHOR INFORMATION

Corresponding Author

*Tel.: +44(0)20 7679 3310. E-mail: d.brett@ucl.ac.uk.

Author Contributions

Electrochemical measurements were performed by N.M. with assistance from X.W., R.J., and C.G. Graphitic carbon nitrides were prepared by A.B.J. with N.M. modifying into fuel cell catalysts. P.F.M., D.B., and F.C. conceived the idea of this study applied to fuel cells. Interpretation and analysis of the data were done with contributions from all authors. N.M., A.B.J., and D.J.L.B. cowrote the manuscript with contributions and comments from the other authors.

Notes

The authors declare no competing financial interest.

ACKNOWLEDGMENTS

The authors acknowledge the EPSRC and UCL Enterprise Impact Acceleration Account (EP/K503745/1) and EPSRC Supergen Fuel Cells (EP/G030995/1) and the EPSRC UK Catalysis Hub (EP/K014706/1) for financial support.

ABBREVIATIONS

PEFCs, polymer electrolyte fuel cells; DOE, U.S. Department of Energy; CNTs, carbon nanotubes; CNFs, carbon nanofibers; CNHs, carbon nanohorns; CNCs, carbon nanocoils; ORR, oxygen reduction reaction; MOR, methanol oxidation reaction; XPS, X-ray photoelectron spectroscopy; CO, carbon monoxide; DMFC, direct methanol fuel cell; DCDA, dicyandiamide; $BmimBF_4$, 1-butyl-3-methylimidazolium tetrafluoroborate; SEM, scanning electron microscopy; TEM, transmission electron microscopy; BET, Brunauer–Emmet–Teller theory; GC, glassy carbon; XRD, X-ray diffraction patterns; ECSA, electrochemical surface area; CV, cyclic voltammogram

REFERENCES

(1) U.S. Department of Energy. Fuel Cell Technologies Program Record: Fuel Cell System Cost, 2012.

(2) U.S. Department of Energy. Fuel Cell Technologies Office Multi-Year Research, Development and Demonstration Plan, 2012. http://www1.eere.energy.gov/hydrogenandfuelcells/mypp/.

(3) Chen, W. X.; Lee, J. Y.; Liu, Z. Microwave-Assisted Synthesis of Carbon Supported Pt Nanoparticles for Fuel Cell Applications. *Chem. Commun.* **2002**, *0*, 2588–2589.

(4) Zhou, J.; Zhou, X.; Sun, X.; Li, R.; Murphy, M.; Ding, Z.; Sun, X.; Sham, T.-K. Interaction between Pt Nanoparticles and Carbon Nanotubes—An X-ray Absorption Near Edge Structures (XANES) Study. *Chem. Phys. Lett.* **2007**, *437*, 229–232.

(5) Shao, Y.; Yin, G.; Wang, Z.; Gao, Y. Proton Exchange Membrane Fuel Cell from Low Temperature to High Temperature: Material Challenges. *J. Power Sources* **2007**, *167*, 235–242.

(6) Sun, X.; Li, R.; Villers, D.; Dodelet, J. P.; Désilets, S. Composite Electrodes Made of Pt Nanoparticles Deposited on Carbon Nanotubes Grown on Fuel Cell Backings. *Chem. Phys. Lett.* **2003**, *379*, 99–104.

(7) Avasarala, B.; Murray, T.; Li, W.; Haldar, P. Titanium Nitride Nanoparticles Based Electrocatalysts for Proton Exchange Membrane Fuel Cells. *J. Mater. Chem.* **2009**, *19*, 1803−1805.
(8) Chhina, H.; Campbell, S.; Kesler, O. An Oxidation-Resistant Indium Tin Oxide Catalyst Support for Proton Exchange Membrane Fuel Cells. *J. Power Sources* **2006**, *161*, 893−900.
(9) Ioroi, T.; Siroma, Z.; Fujiwara, N.; Yamazaki, S.-i.; Yasuda, K. Sub-stoichiometric Titanium Oxide-Supported Platinum Electrocatalyst for Polymer Electrolyte Fuel Cells. *Electrochem. Commun.* **2005**, *7*, 183−188.
(10) Lu, H.; Mu, S.; Cheng, N.; Pan, M. Nano-Silicon Carbide Supported Catalysts for Pem Fuel Cells with High Electrochemical Stability and Improved Performance by Addition of Carbon. *Appl. Catal., B* **2010**, *100*, 190−196.
(11) Rajeswari, J.; Viswanathan, B.; Varadarajan, T. K. Tungsten Trioxide Nanorods as Supports for Platinum in Methanol Oxidation. *Mater. Chem. Phys.* **2007**, *106*, 168−174.
(12) Ruettinger, W.; Liu, X.; Farrauto, R. J. Mechanism of Aging for a Pt/CeO_2−ZrO_2 Water Gas Shift Catalyst. *Appl. Catal., B* **2006**, *65*, 135−141.
(13) Sakurai, H.; Akita, T.; Tsubota, S.; Kiuchi, M.; Haruta, M. Low-Temperature Activity of Au/CeO_2 for Water Gas Shift Reaction, and Characterization by ADF-STEM, Temperature-Programmed Reaction, and Pulse Reaction. *Appl. Catal., A* **2005**, *291*, 179−187.
(14) Sasaki, K.; Zhang, L.; Adzic, R. R. Niobium Oxide-Supported Platinum Ultra-Low Amount Electrocatalysts for Oxygen Reduction. *Phys. Chem. Chem. Phys.* **2008**, *10*, 159−167.
(15) Shen, P. K.; Yin, S.; Li, Z.; Chen, C. Preparation and Performance of Nanosized Tungsten Carbides for Electrocatalysis. *Electrochim. Acta* **2010**, *55*, 7969−7974.
(16) von Kraemer, S.; Wikander, K.; Lindbergh, G.; Lundblad, A.; Palmqvist, A. E. C. Evaluation of TiO_2 as Catalyst Support in Pt−TiO_2/C Composite Cathodes for the Proton Exchange Membrane Fuel Cell. *J. Power Sources* **2008**, *180*, 185−190.
(17) Yin, S.; Mu, S.; Pan, M.; Fu, Z. A Highly Stable TiB_2-Supported Pt Catalyst for Polymer Electrolyte Membrane Fuel Cells. *J. Power Sources* **2011**, *196*, 7931−7936.
(18) Antolini, E. Carbon Supports for Low-Temperature Fuel Cell Catalysts. *Appl. Catal., B* **2009**, *88*, 1−24.
(19) He, D.; Mu, S.; Pan, M. Perfluorosulfonic Acid-Functionalized Pt/Carbon Nanotube Catalysts with Enhanced Stability and Performance for Use in Proton Exchange Membrane Fuel Cells. *Carbon* **2011**, *49*, 82−88.
(20) Hyeon, T.; Han, S.; Sung, Y.-E.; Park, K.-W.; Kim, Y.-W. High-Performance Direct Methanol Fuel Cell Electrodes Using Solid-Phase-Synthesized Carbon Nanocoils. *Angew. Chem., Int. Ed.* **2003**, *42*, 4352−4356.
(21) Sano, N.; Ukita, S.-i. One-Step Synthesis of Pt-Supported Carbon Nanohorns for Fuel Cell Electrode by Arc Plasma in Liquid Nitrogen. *Mater. Chem. Phys.* **2006**, *99* (2−3), 447−450.
(22) Serp, P.; Corrias, M.; Kalck, P. Carbon Nanotubes and Nanofibers in Catalysis. *Appl. Catal., A* **2003**, *253*, 337−358.
(23) Sevilla, M.; Lota, G.; Fuertes, A. B. Saccharide-Based Graphitic Carbon Nanocoils as Supports for PtRu Nanoparticles for Methanol Electrooxidation. *J. Power Sources* **2007**, *171*, 546−551.
(24) Wildgoose, G. G.; Banks, C. E.; Compton, R. G. Metal Nanoparticles and Related Materials Supported on Carbon Nanotubes: Methods and Applications. *Small* **2006**, *2*, 182−193.
(25) Yoshitake, T.; Shimakawa, Y.; Kuroshima, S.; Kimura, H.; Ichihashi, T.; Kubo, Y.; Kasuya, D.; Takahashi, K.; Kokai, F.; Yudasaka, M.; et al. Preparation of Fine Platinum Catalyst Supported on Single-Wall Carbon Nanohorns for Fuel Cell Application. *Physica B: Condens. Mater.* **2002**, *323*, 124−126.
(26) Zhang, S.; Shao, Y.; Yin, G.; Lin, Y. Carbon Nanotubes Decorated with Pt Nanoparticles via Electrostatic Self-Assembly: A Highly Active Oxygen Reduction Electrocatalyst. *J. Mater. Chem.* **2010**, *20*, 2826−2830.
(27) Chang, H.; Joo, S. H.; Pak, C. Synthesis and Characterization of Mesoporous Carbon for Fuel Cell Applications. *J. Mater. Chem* **2007**, *17*, 3078−3088.
(28) Jun, S.; Joo, S. H.; Ryoo, R.; Kruk, M.; Jaroniec, M.; Liu, Z.; Ohsuna, T.; Terasaki, O. Synthesis of New, Nanoporous Carbon with Hexagonally Ordered Mesostructure. *J. Am. Chem. Soc.* **2000**, *122*, 10712−10713.
(29) Machado, B. F.; Serp, P. Graphene-Based Materials for Catalysis. *Catal. Sci. Technol.* **2012**, *2*, 54−75.
(30) Marie, J.; Berthon-Fabry, S.; Chatenet, M.; Chainet, E.; Pirard, R.; Cornet, N.; Achard, P. Platinum Supported on Resorcinol-Formaldehyde Based Carbon Aerogels for PEMFC Electrodes: Influence of the Carbon Support on Electrocatalytic Properties. *J. Appl. Electrochem.* **2007**, *37*, 147−153.
(31) Moreno-Castilla, C.; Maldonado-Hódar, F. J. Carbon Aerogels for Catalysis Applications: An Overview. *Carbon* **2005**, *43*, 455−465.
(32) Selvaganesh, S. V.; Selvarani, G.; Sridhar, P.; Pitchumani, S.; Shukla, A. K. Graphitic Carbon as Durable Cathode-Catalyst Support for PEFCs. *Fuel Cells* **2011**, *11*, 372−384.
(33) Zhou, Y.; Neyerlin, K.; Olson, T. S.; Pylypenko, S.; Bult, J.; Dinh, H. N.; Gennett, T.; Shao, Z.; O'Hayre, R. Enhancement of Pt and Pt-Alloy Fuel Cell Catalyst Activity and Durability via Nitrogen-Modified Carbon Supports. *Energy Env. Sci.* **2010**, *3*, 1437−1446.
(34) Yu, X.; Ye, S. Recent Advances in Activity and Durability Enhancement of Pt/C Catalytic Cathode in PEMFC: Part I. Physico-Chemical and Electronic Interaction between Pt and Carbon Support, and Activity Enhancement of Pt/C Catalyst. *J. Power Sources* **2007**, *172*, 133−144.
(35) Pylypenko, S.; Borisevich, A.; More, K. L.; Corpuz, A. R.; Holme, T.; Dameron, A. A.; Olson, T. S.; Dinh, H. N.; Gennett, T.; O'Hayre, R. Nitrogen: Unraveling the Secret to Stable Carbon-Supported Pt-Alloy Electrocatalysts. *Energy Env. Sci.* **2013**, *6*, 2957−2964.
(36) Yu, X.; Ye, S. Recent Advances in Activity and Durability Enhancement of Pt/C Catalytic Cathode in PEMFC: Part II: Degradation Mechanism and Durability Enhancement of Carbon Supported Platinum Catalyst. *J. Power Sources* **2007**, *172*, 145−154.
(37) Chetty, R.; Kundu, S.; Xia, W.; Bron, M.; Schuhmann, W.; Chirila, V.; Brandl, W.; Reinecke, T.; Muhler, M. PtRu Nanoparticles Supported on Nitrogen-Doped Multiwalled Carbon Nanotubes as Catalyst for Methanol Electrooxidation. *Electrochim. Acta* **2009**, *54*, 4208−4215.
(38) Kundu, S.; Nagaiah, T. C.; Xia, W.; Wang, Y.; Dommele, S. V.; Bitter, J. H.; Santa, M.; Grundmeier, G.; Bron, M.; Schuhmann, W.; et al. Electrocatalytic Activity and Stability of Nitrogen-Containing Carbon Nanotubes in the Oxygen Reduction Reaction. *J. Phys. Chem. C.* **2009**, *113*, 14302−14310.
(39) Lei, Z.; An, L.; Dang, L.; Zhao, M.; Shi, J.; Bai, S.; Cao, Y. Highly Dispersed Platinum Supported on Nitrogen-Containing Ordered Mesoporous Carbon for Methanol Electrochemical Oxidation. *Microporous Mesoporous Mater.* **2009**, *119*, 30−38.
(40) Ozaki, J.-i.; Anahara, T.; Kimura, N.; Oya, A. Simultaneous Doping of Boron and Nitrogen into a Carbon to Enhance its Oxygen Reduction Activity in Proton Exchange Membrane Fuel Cells. *Carbon* **2006**, *44*, 3358−3361.
(41) Wu, G.; Li, D.; Dai, C.; Wang, D.; Li, N. Well-Dispersed High-Loading Pt Nanoparticles Supported by Shell−Core Nanostructured Carbon for Methanol Electrooxidation. *Langmuir* **2008**, *24*, 3566−3575.
(42) Roy, S. C.; Christensen, P. A.; Hamnett, A.; Thomas, K. M.; Trapp, V. Direct Methanol Fuel Cell Cathodes with Sulfur and Nitrogen−Based Carbon Functionality. *J. Electrochem. Soc.* **1996**, *143*, 3073−3079.
(43) Olson, T. S.; Pylypenko, S.; Fulghum, J. E.; Atanassov, P. Bifunctional Oxygen Reduction Reaction Mechanism on Non-Platinum Catalysts Derived from Pyrolyzed Porphyrins. *J. Electrochem. Soc.* **2010**, *157*, B54−B63.
(44) Zhou, Y.; Pasquarelli, R.; Holme, T.; Berry, J.; Ginley, D.; O'Hayre, R. Improving PEM Fuel Cell Catalyst Activity and Durability Using Nitrogen-Doped Carbon Supports: Observations f Model Pt/HOPG Systems. *J. Mater. Chem* **2009**, *19*, 7830−7838.

(45) Sun, C.-L.; Chen, L.-C.; Su, M.-C.; Hong, L.-S.; Chyan, O.; Hsu, C.-Y.; Chen, K.-H.; Chang, T.-F.; Chang, L. Ultrafine Platinum Nanoparticles Uniformly Dispersed on Arrayed CNx Nanotubes with High Electrochemical Activity. *Chem. Mater.* **2005**, *17*, 3749−3753.
(46) Holme, T.; Zhou, Y.; Pasquarelli, R.; O'Hayre, R. First Principles Study of Doped Carbon Supports for Enhanced Platinum Catalysts. *Phys. Chem. Chem. Phys.* **2010**, *12*, 9461−9468.
(47) Wiggins-Camacho, J. D.; Stevenson, K. J. Effect of Nitrogen Concentration on Capacitance, Density of States, Electronic Conductivity, and Morphology of N-Doped Carbon Nanotube Electrodes. *J. Phys. Chem. C.* **2009**, *113*, 19082−19090.
(48) Liebig, J. Uber einige Stickstoff —Verbindungen. *Ann. Pharm.* **1834**, *10*, 1−47.
(49) Franklin, E. C. The Ammono Carbonic Acids. *J. Am. Chem. Soc.* **1922**, *44*, 486−509.
(50) Kroke, E.; Schwarz, M. Novel Group 14 Nitrides. *Coord. Chem. Rev.* **2004**, *248*, 493−532.
(51) Kroke, E.; Schwarz, M.; Horath-Bordon, E.; Kroll, P.; Noll, B.; Norman, A. D. Tri-s-triazine Derivatives. Part I. From Trichloro-tri-s-triazine to Graphitic C_3N_4 Structures. *New J. Chem.* **2002**, *26*, 508−512.
(52) Komatsu, T. Prototype Carbon Nitrides Similar to the Symmetric Triangular Form of Melon. *J. Mater. Chem* **2001**, *11*, 802−803.
(53) Demazeau, G.; Montigaud, H.; Tanguy, B.; Birot, M.; Dunogues, J. The Stabilization of C_3N_4: New Development of Such a Material as Macroscopic Sample. *Rev. High Pressure Sci. Technol.* **1998**, *7*, 1345−1347.
(54) Goglio, G.; Andrault, D.; Courjault, S.; Demazeau, G. Carbon Nitrides: A Promising Class of Materials. *High Pressure Res.* **2002**, *22*, 535−537.
(55) Goglio, G.; Foy, D.; Demazeau, G. State of Art and Recent Trends in Bulk Carbon Nitrides Synthesis. *Mater. Sci. Eng. R. Rep.* **2008**, *58*, 195−227.
(56) Wang, Y.; Zhang, J.; Wang, X.; Antonietti, M.; Li, H. Boron- and Fluorine-Containing Mesoporous Carbon Nitride Polymers: Metal-Free Catalysts for Cyclohexane Oxidation. *Angew. Chem., Int. Ed.* **2010**, *49*, 3356−3359.
(57) Jorge, A. B.; Martin, D. J.; Dhanoa, M. T. S.; Rahman, A. S.; Makwana, N.; Tang, J.; Sella, A.; Corà, F.; Firth, S.; Darr, J. A.; et al. H_2 and O_2 Evolution from Water Half-Splitting Reactions by Graphitic Carbon Nitride Materials. *J. Phys. Chem. C.* **2013**, *117*, 7178−7185.
(58) Kohl, S. W.; Weiner, L.; Schwartsburd, L.; Konstantinovski, L.; Shimon, L. J. W.; Ben-David, Y.; Iron, M. A.; Milstein, D. Consecutive Thermal H_2 and Light-Induced O_2 Evolution from Water Promoted by a Metal Complex. *Science* **2009**, *324*, 74−77.
(59) Liu, H.; Jiang, T.; Han, B.; Liang, S.; Zhou, Y. Selective Phenol Hydrogenation to Cyclohexanone over a Dual Supported Pd−Lewis Acid Catalyst. *Science* **2009**, *326*, 1250−1252.
(60) Su, F.; Mathew, S. C.; Lipner, G.; Fu, X.; Antonietti, M.; Blechert, S.; Wang, X. mpg-C_3N_4-Catalyzed Selective Oxidation of Alcohols Using O_2 and Visible Light. *J. Am. Chem. Soc.* **2010**, *132*, 16299−16301.
(61) Wang, X.; Maeda, K.; Thomas, A.; Takanabe, K.; Xin, G.; Carlsson, J. M.; Domen, K.; Antonietti, M. A Metal-Free Polymeric Photocatalyst for Hydrogen Production from Water Under Visible Light. *Nat. Mater.* **2009**, *8*, 76−80.
(62) Wang, Y.; Di, Y.; Antonietti, M.; Li, H.; Chen, X.; Wang, X. Excellent Visible-Light Photocatalysis of Fluorinated Polymeric Carbon Nitride Solids. *Chem. Mater.* **2010**, *22*, 5119−5121.
(63) Wang, Y.; Wang, X.; Antonietti, M. Polymeric Graphitic Carbon Nitride as a Heterogeneous Organocatalyst: From Photochemistry to Multipurpose Catalysis to Sustainable Chemistry. *Angew. Chem., Int. Ed.* **2012**, *51*, 68−89.
(64) Zheng, Y.; Jiao, Y.; Chen, J.; Liu, J.; Liang, J.; Du, A.; Zhang, W.; Zhu, Z.; Smith, S. C.; Jaroniec, M.; et al. Nanoporous Graphitic-C_3N_4@Carbon Metal-Free Electrocatalysts for Highly Efficient Oxygen Reduction. *J. Am. Chem. Soc.* **2011**, *133*, 20116−20119.
(65) Kim, M.; Hwang, S.; Yu, J.-S. Novel Ordered Nanoporous Graphitic C_3N_4 as a Support for Pt−Ru Anode Catalyst in Direct Methanol Fuel Cell. *J. Mater. Chem* **2007**, *17*, 1656−1659.
(66) Mansor, N.; Belen Jorge, A.; Corà, F.; Gibbs, C.; Jervis, R.; McMillan, P. F.; Wang, X.; Brett, D. J. L. Development of Graphitic-Carbon Nitride Materials as Catalyst Supports for Polymer Electrolyte Fuel Cells. *ECS Trans.* **2013**, *58*, 1767−1778.
(67) Wirnhier, E.; Döblinger, M.; Gunzelmann, D.; Senker, J.; Lotsch, B. V.; Schnick, W. Poly(triazine imide) with Intercalation of Lithium and Chloride Ions $[(C_3N_3)_2(NH_xLi_{1-x})_3{\cdot}LiCl]$: A Crystalline 2D Carbon Nitride Network. *Chem.—Eur. J.* **2011**, *17*, 3213−3221.
(68) Bojdys, M. J.; Müller, J.-O.; Antonietti, M.; Thomas, A. Ionothermal Synthesis of Crystalline, Condensed, Graphitic Carbon Nitride. *Chem.— Eur. J.* **2008**, *14*, 8177−8182.
(69) Bleda-Martínez, M. J.; Maciá-Agulló, J. A.; Lozano-Castelló, D.; Morallón, E.; Cazorla-Amorós, D.; Linares-Solano, A. Role of Surface Chemistry on Electric Double Layer Capacitance of Carbon Materials. *Carbon* **2005**, *43*, 2677−2684.
(70) Young, A. P.; Stumper, J.; Gyenge, E. Characterizing the Structural Degradation in a PEMFC Cathode Catalyst Layer: Carbon Corrosion. *J. Electrochem. Soc.* **2009**, *156*, B913−B922.
(71) Garsany, Y.; Baturina, O. A.; Swider-Lyons, K. E.; Kocha, S. S. Experimental Methods for Quantifying the Activity of Platinum Electrocatalysts for the Oxygen Reduction Reaction. *Anal. Chem.* **2010**, *82*, 6321−6328.
(72) Mayrhofer, K. J. J.; Arenz, M.; Blizanac, B. B.; Stamenkovic, V.; Ross, P. N.; Markovic, N. M. CO Surface Electrochemistry on Pt-Nanoparticles: A Selective Review. *Electrochim. Acta* **2005**, *50*, 5144−5154.
(73) Mayrhofer, K. J. J.; Blizanac, B. B.; Arenz, M.; Stamenkovic, V. R.; Ross, P. N.; Markovic, N. M. The Impact of Geometric and Surface Electronic Properties of Pt-Catalysts on the Particle Size Effect in Electrocatalysis. *J. Phys. Chem. B* **2005**, *109*, 14433−14440.